An Easily Extendable FFT Based Four-Channel, Four-Beam Receiver With Progressive Partial Spatial Filtering in 65nm

Qingrui Meng and Ramesh Harjani
University of Minnesota, Minneapolis, MN 55455, USA. Email: harjani@umn.edu

***Abstract*—This paper presents a novel four-channel, four-beam receiver core based on a FFT core that is easily extended to a larger number of beams. This architecture is particulary well suited for MIMO systems where multiple beams are used for increased throughput. Like the FFT, the proposed architecture reuses computations for multi-beam systems. In particular, the proposed architecture redistributes the computations so as to maximize the reuse of the structure that already exist in a receiver chain. In many fashions the architecture is quite similar to a Butler matrix but unlike the Butler matrix it does not use large passive components at RF. Further, we exploit the normally occurring quadrature down-conversion process to implement the tap weights. In comparison to traditional MIMO architectures, that effectively duplicate each path, the distributed computations of this architecture provide partial spatial filtering before the final stage, improving interference rejection for the blocks between the LNA and the ADC. Additionally, because of the spatial filtering prior to the ADC, a single interferer only jams a single beam allowing for continued operation though at a lower combined throughput. The four-beam receiver core prototype in 65nm CMOS implements the basic FFT based architecture but does not include an LNA or extensive IF stages. This four-channel design consumes 56mW power and occupies an active area of $0.65mm^2$ excluding pads and test circuits.**

***Keywords*—Butler matrix, FFT, multi-beam, phased array, beamforming, multiple-input-multiple-output (MIMO), spatial filter**

I. Introduction

Multipath interference plays a significant role in limiting wireless system performance. Multi-input and multi-output (MIMO) transceivers can reduce its adverse effects by increasing diversity and multiplexing gain, leading to increased throughput. Digital beamforming offers more flexibility but requires a large ADC dynamic range.

RF phased arrays provide the flexibility of electronic beam steering but rapidly become complex for multi-beam systems. The Butler matrix can more efficiently provide multiple fixed beams [1] by sharing common computations in a manner quite analogous to FFT implementations of the discrete Fourier transform [2]. Let us consider a four-channel, simultaneous four-beam architecture as an example, sixteen phase shifters are needed for the phased array, but only four hybrids and two 45° phase shifters are needed for the Butler matrix [3]. The savings increase as the number of beams and antennas increase. Our proposed architecture inherits this computational advantage due to the similarity between the Butler matrix and the FFT [4]. In [5] a Butler matrix is placed right after the LNAs, and the spatially filtered RF outputs (usually at $-48.6^\circ, -14.4^\circ, +14.4^\circ \text{and} +48.6^\circ$) are then down-converted by mixers. One of the advantages of the passive Butler matrix is that spatial filtering is performed close to the antenna. However, passive Butler matrices tend to be physically bulky, and are not well suited for integrated environments. Significant research has focused on using different implementations for the passive components to reduce size [6], [7].

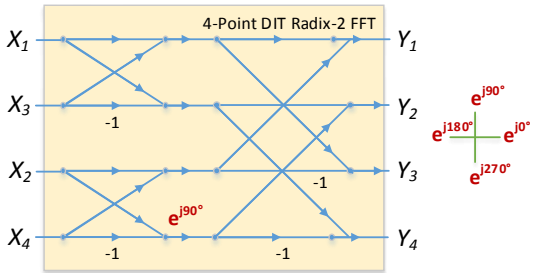

Fig. 1: Decimation-in-time 4-point FFT

This paper describes a FFT based RF/analog four-channel four-beam receiver that *more efficiently exploits existing receiver components for simultaneous multi-beam generation*. Section II presents the system architecture. Section III describes the circuit designs and Section IV shows the measurement results. Section V concludes the paper.

II. Proposed Architecture

A. Proposed four-channel four-beam receiver

Before we consider the actual architecture let us consider the set of four DFT equations, Eqns (1)-(4).

$$Y_1 = X_1 e^{j0^\circ} + X_2 e^{j0^\circ} + X_3 e^{j0^\circ} + X_4 e^{j0^\circ} \quad (1)$$
$$Y_2 = X_1 e^{j0^\circ} + X_2 e^{j90^\circ} + X_3 e^{j180^\circ} + X_4 e^{j270^\circ} \quad (2)$$
$$Y_3 = X_1 e^{j0^\circ} + X_2 e^{j180^\circ} + X_3 e^{j0^\circ} + X_4 e^{j180^\circ} \quad (3)$$
$$Y_4 = X_1 e^{j0^\circ} + X_2 e^{j270^\circ} + X_3 e^{j180^\circ} + X_4 e^{j90^\circ} \quad (4)$$

The output quantities Y_1, Y_2, Y_3 and Y_4 are equal to the sum of four-channel inputs, (X_1, X_2, X_3 and X_4) phased rotated by 0°, 90°, 180° and 270° respectively. The associated FFT signal flow is shown in Fig. 1. We note that phase rotation of 0° and 180° can easily be done in the current domain with differential signals. We also note that a normal receiver uses quadrature down-conversion with I and Q LO signals. So, using a differential implementation the 90° and 270° signals are readily available at IF. The details are discussed next.

The proposed four-channel, four-beam receiver is shown in Fig. 2. The four antenna inputs are fed through external LNAs, then these signals are pairwise ($1 : \pm 1$) combined [added (0°) or subtracted (180°)] in the current domain before down-conversion. In particular, at RF the channels associated with X_1 and X_3 form a pair, and X_2 and X_4 form the second pair using the reverse binary for a decimation-in-time FFT. The RF signals are then down-converted to IF where the final stage of signal combination is done. Considering Y_1 and Y_3 as examples, Y_1 uses the sum of mixer outputs associated with X_1 and X_2, and Y_3 uses the difference of the mixer outputs associated with X_1 and X_2. Note that for only the 4^{th} channel the I+I- and Q+Q- are replaced by Q+Q-

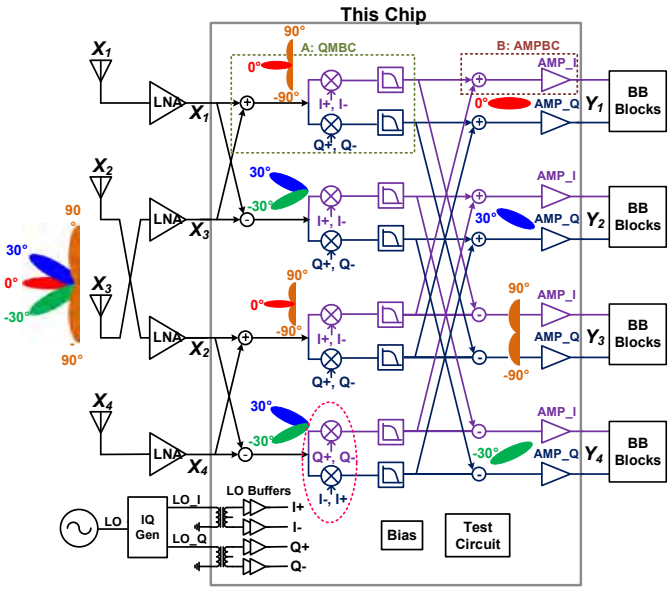

Fig. 2: Proposed four-channel four-beam receiver

and I-I+ which is nothing but a phase rotation of 90°. The additions and subtractions at IF are also easily accomplished in the current domain. All the computations discussed directly utilize pre-existing components of a receiver (other than signal swapping and signal routing) without adding additional stages.

The input phase rotation of 0°, 90°, 180° and 270° indicated by Eqns (1)-(4) yield 0°, +30°, ±90° and −30° spatial beam directions as shown in Fig. 2, in comparison to the −14.4°, −48.6°, 48.6° and 14.4° beam directions for a Butler matrix, using a $\lambda/2$ antenna distance.

B. Partial spatial filtering

Because some of spatial filtering is done at RF our design inherits properties of both RF beamforming and IF beamforming without the difficulty of realizing all the beams at RF. Signal addition (0°), subtraction (180°) and (90°) and (270°) phase shifting could in theory all be accomplished in the baseband [8]. However, it would not provide the partial spatial filtering shown in Fig. 2. Note, the beam-width is given by $\lambda/(Nd)$, where N is the number of antennas, and d is the distance between adjacent antennas [3]. In our design, there are $\log_2(4) = 2$ combining stages. The first signal combining at the mixer input forms a two-channel phased array with an adjacent antenna distance of λ. In this case two grating-lobes show up due to the λ spacing. The RF signal combining provides "partial spatial filtering" of interference close to the main-lobe and improves the jammer rejection for all the blocks that follow it. The broadside array patterns for a 4-channel is shown in Fig. 3 (a). The red lines show the "partial spatial filtering" after the RF combiner and the blue dots show the final beam. The main lobe remains the same and only parasitic grating-lobes show up due to the larger antenna spacing.

C. Increasing the number of channels and beams

In a manner similar to a Butler matrix or FFT, higher order architectures can be recursively constructed from smaller designs by adding additional finer phase resolution trellises which are much easier to implement at IF with I and Q signals [2]. For example, the 8-point FFT shown in Fig. 4 basically consists of two parallel 4-point FFTs that is followed

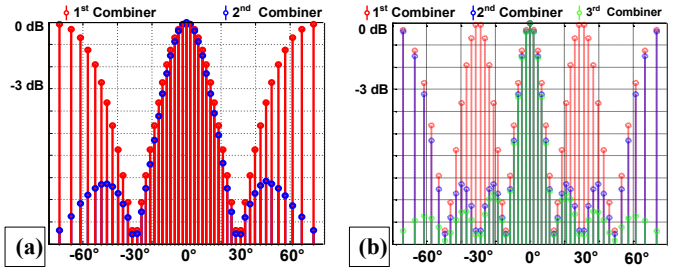

Fig. 3: Partial spatial filtering for (a) 4-channels and (b) 8-channels

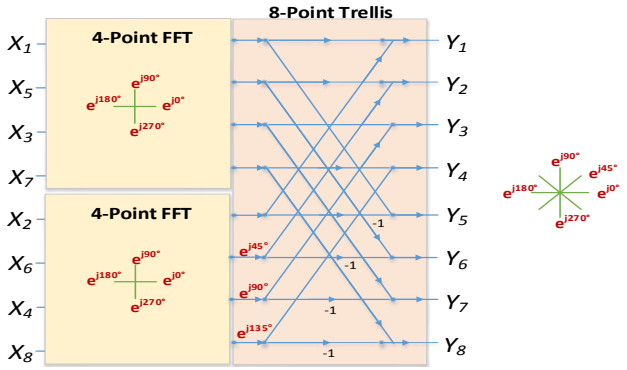

Fig. 4: 8-point FFT = two 4-point FFTs + 8-point trellis

by an 8-point trellis. The 8-point trellis requires $360°/8 = 45°$ phase resolution, which is much easier to implement at IF once I and Q signals are available after down conversion.

The 8-point trellis differs from a fixed multi-beam IF phased array. In particular, not unlike in an FFT, the 8-point trellis reuses computations to generate the simultaneous eight beams in comparison to an IF phased array. Table I shows a comparison of computations required for a fixed IF phased-array and our architecture. (Note: the phase rotator design is more complicated for a steerable array.) For the 4-beam design the combiners only use addition or negation either at RF or at IF. For the 8-beam design we use a cartesian combination of equal values of I and Q signals to realize the 45° angles. In a similar fashion, a 16-beam system would utilize two 8-beam systems and an additional 16-point trellis.

Partial spatial filtering is present in higher number of channels as well. The main-lobe remains the same while the grating-lobes get progressively smaller as we get closer to the ADC. The 8-channel case is shown in Fig. 3 (b) where the second combiner, in blue, does not have the lobes at ±30° that were present for the first combiner, in red. The final narrow beam is shown in green.

III. Circuit Design

All circuit implementations are fully differential but only simplified versions are shown for clarity. Four single-ended RF signals are introduced on-chip using GSGSG probes and differential versions are generated using on-chip baluns. In a similar fashion differential versions of LO-I and LO-Q are generated using on-chip baluns. In particular, we describe A:QMBC and B:AMPBC shown within the inset of Fig. 2.

TABLE I: COMPUTATIONS COMPARISON

		IF phased array		Our architecture	
♯ of Combiners	IF	$8 \times 2 = 16$	8 inputs	$16 \times 2 = 32$	2 inputs
	RF	–		$4 \times 2 = 8$	2 inputs
♯ of Rotators		$8 \times 7 \times 2 = 112$		$3 \times 2 = 6$	

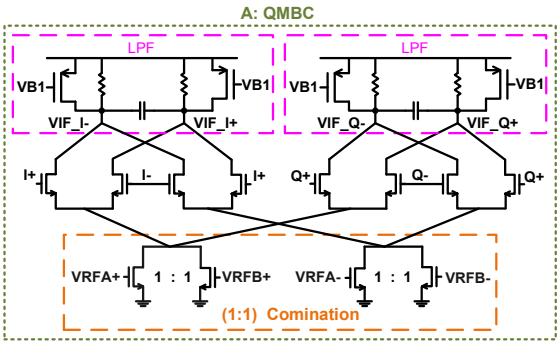

Fig. 5: Quadrature mixer with built-in combiner (QMBC)

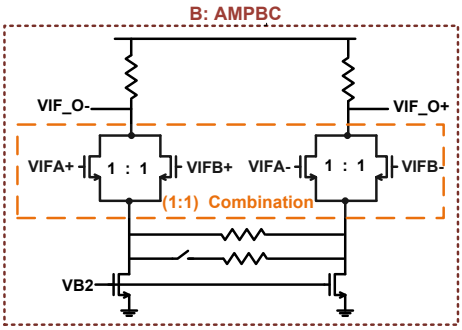

Fig. 6: Amplifier with built-in combiner (AMPBC)

A. *Quadrature mixer with built-in combiner (QMBC)*

The quadrature mixer with built-in combiner (QMBC) is based on a traditional double-balanced Gilbert cell topology and is shown in Fig. 5. The RF signal $(1:1)$ combination (or addition) is realized using RF tail transistors with differential signals $VRFA\pm$ and $VRFB\pm$ from the two channels. The output current is then evenly distributed between the I and Q paths, and down-converted and low pass filtered to $VIF\_I\mp$ and $VIF\_Q\mp$. In a similar fashion, the negative QMBC output is generated by interchanging the input connection to $VRFB+$ and $VRFB-$ to achieve $(1:-1)$ combination (or subtraction). The LO switches have minimum lengths to reduce loading of the LO drivers. The composite PMOS and resistor output load was sized to provide good noise performance. Note, that the RF tail transistor is split into two for each channel and the total mixer current remains the same as would have been for completely separate channels.

B. *Amplifier with built-in combination(AMPBC)*

Similarly, the $(1:1)$ combination can be implemented directly at the IF amplifier inputs, where differential signals from two channel $VIFA\pm$ and $VIFB\pm$ are combined as shown in Fig. 6. This circuit is based on a source degenerated common source amplifier optimized for linearity and phase accuracy. The $(1:-1)$ combination is realized by switching connections between $VIFB+$ and $VIFB-$. The length of the combination transistors are sized larger to reduce the phase error, since its loading effect at IF is less critical. No additional current is used here either.

IV. Measurements

For this first prototype a complete receiver chain was not realized to limit risk while illustrating the design principles. We did not include an LNA or extensive IF stages. However, the critical beamforming blocks for the proposed architecture was implement by slightly modifying pre-existing receiver

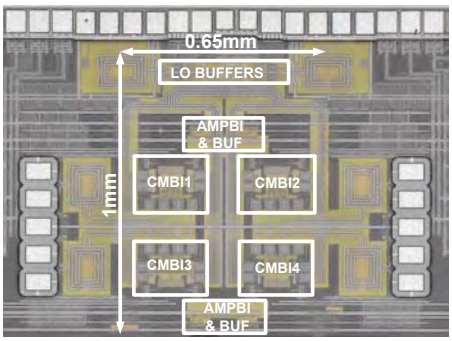

Fig. 7: Chip micrograph

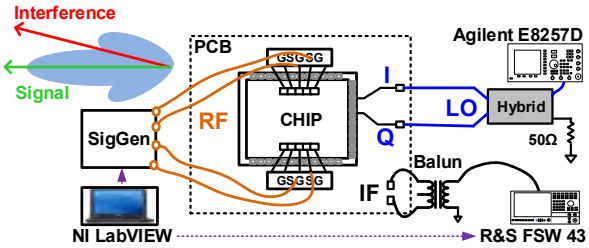

Fig. 8: Measurement setup

components. The micrograph for the chip fabricated in TSMC's 65nm GP CMOS process is shown in Fig. 7. The active area (excluding test circuits) is $0.65mm^2$. The four channel receiver draws 55mA current from a 1V power supply, and the LO buffers consume 23mA. Note, all baluns in Fig. 7 are included for testing purposes only.

The measurement setup for array characterization is shown in Fig. 8. For initial testing 4-channel CW signals were generated by Labview control of a 4-port Rohde&Schwarz ZVA 67 network analyzer. The four channel signals are input to the chip via two GSGSG probes. On-chip 50Ω resistors and baluns (not shown in Fig. 2) are placed at RF inputs to provide termination and to convert the signals from single-ended to differential. The 7.78GHz LO signal is provided by an Agilent E8257D, power-split into I and Q by an off-chip hybrid, and fed via bond wires to the chip. A balun converts the LO signals into differential. The four-channel IF outputs are connected to a Rohde&Schwarz FSW43 Spectrum Analyzer via an off-chip balun to measure the signal power at Y_1, Y_2, Y_3 and Y_4. For array pattern measurement, the ZVA was set up in coherence mode. The measured normalized array patterns with 5° measurement steps, for the four-channel outputs at different input phases are shown in Fig. 9. Consider the output at Y_1 as an example: here a broadside beam at 0° is constructed, while signals at spatial angle of $+30^\circ$, $\pm 90^\circ$ and -30° are nulled out. The measured null-depths for 30°, -30° and $\pm 90^\circ$ spatial angles are 24.5dB, 26.2dB and 23.4dB respectively. The other beams at spatial angle of 30°, -30° and $\pm 90^\circ$ have similar results. The measured null-depths is always better than 19dB, is limited by the phase balance of the off-chip hybrid. Measured RF bandwidth is 2.5GHz centered at 7.8GHz. Single channel noise figure for this design does not translate easily to multi-beam designs.

Next, we test the system EVM with and without interference nulling. The setup remains the same except we send composite signals for all four channels. The desired modulated signal, generated via a Rohde&Schwarz SMW vector signal generator, is provided broadside at 7.8GHz. The interference signal, generated via the another port of

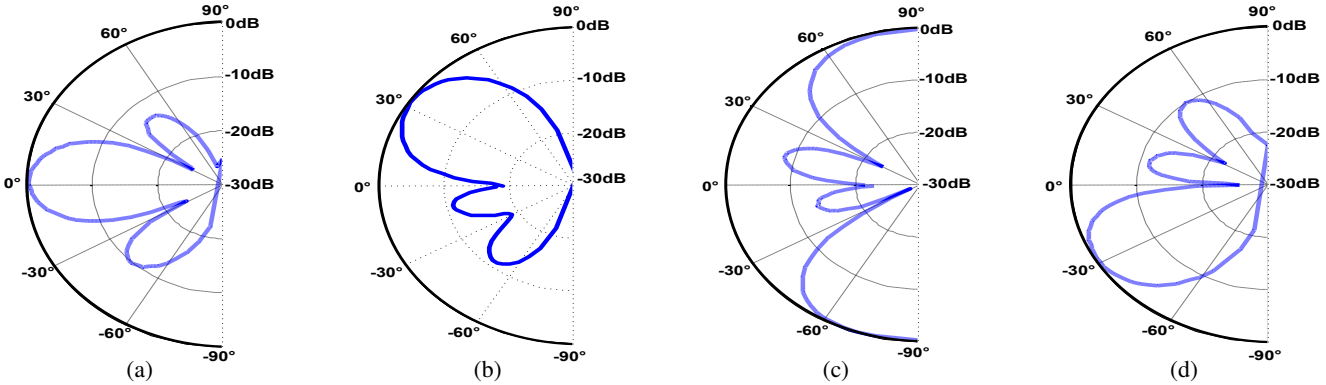

(a) (b) (c) (d)

Fig. 9: Measured normalized array patterns for the receiver at (a) Y_1, broadside, (b) Y_2, $+30°$, (c) Y_3, end-fire, and (d) Y_4, $-30°$

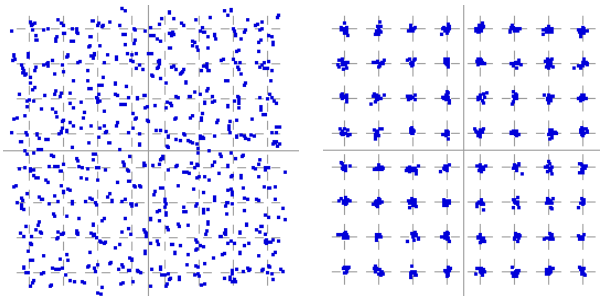

(a) EVM=11.15% (b) EVM=3.17%

Fig. 10: Measured constellations (a) without and (b) with interference nulling

TABLE II: PERFORMANCE COMPARISON

Ref. No.	Tech. (nm)	Beam No.	Area (mm^2)	Cent. Freq. (GHz)	Loss (dB)	Null-depth (dB)
[5]	90	4	14.28	25	>2-4[1]	—
[6]	130	8	4.75	5.5	3.5[2]	—
[7]	65	4	0.072[3]	63	2.77	>17
This work	**65**	**4**	**0.65**	**7.8**	**—**	**>19**[4]

[1]The hybrid loss is 1-2dB [9]. [2]By simulation. [3]Higher operation frequency. [4]Can be improved by calibration.

the SMW, is provided once at broadside and once at 30°. The measured EVM for the 64QAM 1MS/s broadside beam, i.e., without interference nulling, at Y_1 is 11.15% as shown in Fig. 10a. While the measured EVM for the same beam when the interference is at 30° is 3.17% showing the benefit of interference nulling. In comparison the EVM with no interference is 1.12%.

In a normal MIMO system we use the information from all four antennas. Our design, that has spatial filtering is also capable of supporting a full MIMO system as the original 4 antenna signals can be reconstructed using a I-FFT in the digital domain. However, the proposed design has a significant advantage over four independent channels. In the case of four independent channels a single interference would overload all four channels. However, as seen in the last experiment, the proposed design is still able to provide functionality, though at a lower effective throughput, as long as the number of interferers is less than the number of beams.

The performance comparison is summarized in Table II. A direct comparison with other designs is not straightforward, as Butler matrix publications typically remain at RF. References [5], [6] do not specify null-depths, but was estimated from the array patterns and is limited to 20dB worst case. The closest comparison [5] implements a full MIMO system based on a Butler matrix. We have developed an easily extendable design with partial spatial filtering.

V. Conclusions

In this work, a new four-channel four-beam receiver architecture with built-in beamforming by reusing existing blocks in receiver is reported. Analogous to an FFT, the design utilizes shared computations to generate four simultaneous beams with improved performance, including: a) Removal of large passive components to realize the multiple beams; b) Utilizing distributed computations (including signal combinations and phase shifting) resulting in partial spatial filtering from RF to IF resulting in better interference tolerance in comparison to IF beam forming; c) Uses larger phase steps than a Butler matrix. For example, a four-beam Butler matrix needs 45° phase resolution, while our design needs 90° resolution; d) Higher order beams can be formed by combining multiple lower order systems. The connection between Butler matrix, FFT and phased arrays are well know. However, we have exploited the architecture of integrated receivers to reduce the number and complexity of phase rotators and combiners. The savings increase as the number of channels increase.

Acknowledgement: Funded by the DARPA CLASIC program.

References

[1] J. Butler and R. Lowe, "Beam forming matrix simplifies design of electronically scanned antennas," *Electronic Design*, pp. 170–173, Apr. 1961.

[2] A. V. Oppenheim and R. W. Schafer, *Discrete-Time Signal Processing*. Prentice Hall, 2009.

[3] R. J. Mailloux, *Phased Array Antenna Handbook*. Artech House, 2005.

[4] J. P. Shelton, "Fast Fourier transforms and Butler matrices," *Proceedings of The IEEE*, vol. 56, p. 350, Mar. 1968.

[5] H. Krishnaswamy and H. Hashemi, "A 4-channel, 4-beam, 24-26GHz, spatio-temporal RAKE radar transceiver in 90nm CMOS for vehicular radar applications," in *IEEE International Solid State Circuits Conference*, Feb. 2010, pp. 214–215.

[6] B. Cetinoneri, Y. A. Atesal, and G. M. Rebeiz, "An 8x8 Butler matrix in 0.13-μm CMOS for 5-6-GHz multibeam applications," *IEEE Trans. Microwave Theory Tech*, vol. 59, p. 295301, Feb. 2011.

[7] T. C. Jong Seok Park and H. Wang, "An Ultra-Broadband Compact Mm-Wave Butler Matrix in CMOS for Array-Based MIMO Systems," in *Custom Integrated Circuits Conference*, Sep. 2013.

[8] F. Rivet *et al.*, "The Experimental Demonstration of a SASP-Based Full Software Radio Receiver," in *IEEE Journal of Solid-State Circuits*, May 2010, pp. 979–988.

[9] H. Krishnaswamy, "Architecture and integrated circuits for RF and mm-wave multiple-antenna systems on silicon," in *University of Southern California Dissertations and Theses*, 2009.